12th International Conference on Applications of Statistics and Probability in Civil Engineering, ICASP12
Vancouver, Canada, July 12-15, 2015

Stochastic Multi-scale Finite Element Analysis for Laminated Composite Plates

Xiao-Yi Zhou
Research Associate, School of Civil Engineering and Geosciences, Newcastle University, Newcastle upon Tyne, UK

Peter D. Gosling
Professor, School of Civil Engineering and Geosciences, Newcastle University, Newcastle upon Tyne, UK

ABSTRACT: This paper proposes a dual stochastic finite element method for conducting stochastic analysis for laminated composite plates with consideration of microscopic material property uncertainties. A stochastic multiscale finite element method, which couples the multiscale computation homogenization method with the second order perturbation technique, is developed first to propagate variability in the effective elasticity property of composite arising from microscopic uncertainties such as Young's modulus and Poisson's ratio of constituent materials. Then a standard stochastic finite element analysis is conducted to consider structural level uncertainties. The performance of the proposed approach is evaluated by comparing the estimates of mean values and coefficients of variation for the effective elastic properties and structural response for a laminated composite plate with corresponding results from the Monte Carlo simulation method.

1. INTRODUCTION

Composite materials are becoming increasingly important in civil engineering applications where the tailoring opportunities offered by composite fibre reinforcement can achieve engineering requirements not attainable by conventional steel and concrete options. Enormous efforts have been devoted to predict the effective mechanical properties of composite materials to advance the structural analysis for composite structures in deterministic context. However, it has been widely accepted and extensively reported that uncertainties exist in all aspects of a composite structure, e.g. constituent material properties, that result in uncertainties in structural responses. Due to the heterogeneous nature of composites, the uncertain behaviour in performance of a composite structure such as laminated plate is often more higher than the conventional isotropic material structures. An efficient and accurate quantification of the uncertainty in structural performance is thus desirable to analyse a composite structure, and it is also a crucial part of the development of reliability-based design method for composite structures.

The objectives to quantitative modelling of uncertainty of systems with random properties can be divided into three groups: the description of the random properties of the system (Jeong and Shenoi, 2000; Chuang, 2006), the calculation of statistical information of the response from the system properties (Motley and Young, 2011; Sasikumar et al., 2014; Talha and Singh, 2014), and the interpretation and use of this statistical response information for design, maintenance, repair, and so on (Murotsu et al., 1994; Frangopol and Recek, 2003; Soares, 1997). The calculation of the statistical response characteristics requires an extension of the traditional deterministic analysis that leads to stochastic analysis. Monte Carlo simulation method, perturbation method and spectral method

are the available solutions for this type of problem (Matthies, 2007; Schuëller and Pradlwarter, 2009; Stefanou, 2009). Although stochastic finite element based methods have been used for a long time, it is only recently that attempts are being made to extend these methods for uncertainty quantification in composite materials and composite structures (Chen and Guedes Soares, 2008; Ngah and Young, 2007; Talha and Singh, 2014). However, most of previous work on stochastic analysis for laminated composite plates focused on meso-scale uncertainties such as ply or lamina material properties. For instance, Chen and Guedes Soares (2008) consider the uncertainty of Young's modulus. Ngah and Young (2007) considered the components in the constitutive stiffness matrix as random field. Many studies have shown that mechanical properties of multi-phase composite materials are strongly affected by their microscopic heterogeneous nature (Sriramula and Chryssanthopoulos, 2009; Potter et al., 2008). Various of homogenization methods are available in the literature to predict effective material properties of composites. Although it has been pointed out that potential benefits can be obtained (Charmpis et al., 2007), considerations on microscopic material property uncertainties, especially through micromechanics method, are seldom reported in stochastic analysis. Chamis (2004) and Welemane and Dehmous (2011) are a few that investigated microscopic uncertainties for stochastic analysis of composite structures.

In order to taking microscopic uncertainties into account in stochastic analysis of composite structures, this paper presents a dual stochastic finite-element based procedure. Among the many inherent uncertainties, we mainly focus on microscopic constituent material properties in present study. The analytical development starts with the propagation of uncertainties at the microscopic material properties to determine the effective material properties at macro or ply scale by using the stochastic homogenization method (Zhou et al., 2014). First-order shear deformation laminate theory is then used as basis to propagate the uncertainty in the material behaviour at the laminate or structural scale. Next, the stochastic finite element analysis is performed to determine the stochastic structural responses corresponding to the uncertain basic variables. A case study of laminated composite plate is performed to illustrate the proposed method for the analysis of composite structures.

2. Stochastic variational formulation of multiscale approach

2.1. *Stochastic homogenization method for composite materials*

First, we will summarize the basic assumptions and the final formulae of the stochastic homogenization method for the estimation of effective elastic moduli. For a detailed discussion and numerous references for this and related methods, the reader is referred to Zhou et al. (2014). The class of homogenization-based multi-scale constitutive models employed in the present study is characterised by the assumption that the strain and stress tensors at a point of the so-called macro-continuum are volume average of their respective microscopic counterpart fields over a pre-specified Representative Volume Element (RVE). That is, by defining the deformation gradient $\bar{\varepsilon}$ and the stress tensor $\bar{\sigma}$ as volume averages of their counterpart fields over the RVE, we have

$$\bar{\varepsilon} \equiv \frac{1}{V_\mu}\int_{\Omega_\mu} \varepsilon_\mu dV = \frac{1}{V_\mu}\int_{\Omega_\mu} \nabla \mathbf{u}_\mu dV \qquad (1)$$

and

$$\bar{\sigma} = \frac{1}{V_\mu}\int_{\Omega_\mu} \sigma_\mu dV \qquad (2)$$

where ε_μ and σ_μ denote, respectively, the deformation gradient and the stress fields of the RVE, V_μ is the volume of the RVE and ∇ denotes the gradient operator.

By defining the field $\tilde{\mathbf{u}}_\mu$ of displacement fluctuations of the RVE as

$$\tilde{\mathbf{u}}_\mu \equiv \mathbf{u}_\mu - \mathbf{u}^* \quad \text{with} \quad \mathbf{u}^* = \bar{\varepsilon}\mathbf{y} \qquad (3)$$

The deformation gradient field of the RVE can be written as a sum of a uniform deformation gradient coinciding with the macroscopic deformation gradient, $\bar{\varepsilon}$, and a displacement fluctuation gradient field, $\tilde{\varepsilon} \equiv \nabla\tilde{\mathbf{u}}_\mu$,

$$\varepsilon_\mu = \bar{\varepsilon} + \tilde{\varepsilon} \qquad (4)$$

To comply with the averaging strain assumption, the displacement fluctuation field must satisfy

$$\int_{\Omega_\mu} \tilde{\varepsilon}_\mu dV = \mathbf{0}. \tag{5}$$

To make upscaling transition, a second assumption also known as the Hill-Mandel principle is introduced, and it requires

$$\bar{\sigma} : \bar{\varepsilon} = \frac{1}{V_\mu} \int_{\Omega_\mu} \sigma_\mu : \varepsilon_\mu dV \tag{6}$$

Considering the RVE equilibrium and the second assumption, it introduces an addition constraint for the RVE that requires:

$$\int_{\partial\Omega_\mu} \mathbf{t}^e \cdot \eta dA = 0 \quad \eta \in \mathscr{V}, \tag{7}$$

in terms of the RVE boundary traction $\mathbf{t}^e$.

Hence, the RVE equilibrium problem for a linear-elastic material case consists of finding, for a given macroscopic deformation $\bar{\varepsilon}$, a kinematically admissible displacement fluctuation field $\tilde{\mathbf{u}}_\mu \in \mathscr{V}$ under constraints Eqs.(5) and (7), such that

$$\int_\Omega \sigma : \nabla\eta dV = \int_\Omega \left(\mathbb{C}_\mu \varepsilon_\mu\right) : \nabla\eta dV = 0 \quad \forall\eta \in \mathscr{V}, \tag{8}$$

where $\mathbb{C}_\mu$ is material constitutive tensor and $\mathscr{V}$ is the (as yet not defined) space of virtual kinematically admissible displacement of the RVE.

Considering the uncertainties in material properties, $\mathbf{b}$, constitutive matrix $\mathbb{C}_\mu$ and displacement fluctuation $\tilde{\mathbf{u}}_\mu$ are stochastic function of $\mathbf{b}$. Using perturbation method, the variational function Eq.(8) can be transformed into its zeroth-, first- and second-order approximations as:

- The zeroth order

$$\int_{\Omega_\mu^s} \nabla^s\eta : \mathbb{C}_\mu(\bar{\mathbf{b}}) : \nabla^s\tilde{\mathbf{u}}_\mu(\bar{\mathbf{b}}) dV + \int_{\Omega_\mu^s} \nabla^s\eta : \mathbb{C}_\mu(\bar{\mathbf{b}}) : \varepsilon dV = 0 \tag{9}$$

- The first-order

$$\sum_{p=1}^{n} \left\{ \int_{\Omega_\mu^s} \nabla^s\eta : \left(\mathbb{C}_\mu(\bar{\mathbf{b}}) : \left[D_{b_p}\nabla^s\tilde{\mathbf{u}}_\mu(\bar{\mathbf{b}})\right] + \left[D_{b_p}\mathbb{C}_\mu(\bar{\mathbf{b}})\right] : \nabla^s\tilde{\mathbf{u}}_\mu(\bar{\mathbf{b}})\right) dV + \int_{\Omega_\mu^s} \nabla^s\eta : \left[D_{b_p}\mathbb{C}_\mu(\bar{\mathbf{b}})\right] : \varepsilon dV \right\} \delta b_p = 0 \tag{10}$$

- The second-order

$$\sum_{p=1}^{n}\sum_{q=1}^{n} \left\{ \int_{\Omega_\mu^s} \nabla^s\eta : \left(\mathbb{C}_\mu(\bar{\mathbf{b}}) : \left[H_{b_pb_q}\nabla^s\tilde{\mathbf{u}}_\mu(\bar{\mathbf{b}})\right] + \left[H_{b_pb_q}\mathbb{C}_\mu(\bar{\mathbf{b}})\right] : \nabla^s\tilde{\mathbf{u}}_\mu(\bar{\mathbf{b}}) + 2\left[D_{b_p}\mathbb{C}_\mu(\bar{\mathbf{b}})\right] : \left[D_{b_q}\nabla^s\tilde{\mathbf{u}}_\mu(\bar{\mathbf{b}})\right]\right) dV + \int_{\Omega_\mu^s} \nabla^s\eta : \left[H_{b_pb_q}\mathbb{C}_\mu(\bar{\mathbf{b}})\right] : \varepsilon dV \right\} \delta b_p \delta b_q = 0 \tag{11}$$

2.2. Stochastic formulation for laminated composite plates

In this section, the stochastic variational formulation for probabilistic analysis of laminated composite plates is deduced by the first-order or Reissner-Mindlin shear deformation theory (FSDT) and the perturbation method. Using FSDT the displacement components u, v and w can be expressed in terms of the mid-plane displacements u_0, v_0, w_0, and the rotations of transverse normal about y- and x-axes of θ_x and θ_y, respectively, as (details in Oñate (2013) for example)

$$\begin{aligned} u(x,y,z) &= u_0(x,y) - z\theta_x(x,y) \\ v(x,y,z) &= v_0(x,y) - z\theta_y(x,y) \\ w(x,y,z) &= w_0(x,y) \end{aligned} \tag{12}$$

The strain components are computed using the above displacement field with $\varepsilon = \nabla\mathbf{u}$, and it is expressed as

$$\varepsilon = \begin{pmatrix} \varepsilon_m & \mathbf{0} \end{pmatrix}^T + \begin{pmatrix} -z\hat{\varepsilon}_b & \hat{\varepsilon}_s \end{pmatrix}^T = \mathbf{S}\hat{\varepsilon} \tag{13}$$

where

$$\hat{\varepsilon} = \begin{pmatrix} \hat{\varepsilon}_m & \hat{\varepsilon}_b & \hat{\varepsilon}_s \end{pmatrix}^T \tag{14}$$

with

$$\begin{aligned} \hat{\varepsilon}_m &= \left[\frac{\partial u_0}{\partial x}, \frac{\partial v_0}{\partial y}, \left(\frac{\partial u_0}{\partial y} + \frac{\partial v_0}{\partial x}\right)\right]^T \\ \hat{\varepsilon}_b &= \left[\frac{\partial \theta_x}{\partial x}, \frac{\partial \theta_y}{\partial y}, \left(\frac{\partial \theta_x}{\partial y} + \frac{\partial \theta_y}{\partial x}\right)\right]^T \\ \hat{\varepsilon}_s &= \left[\frac{\partial w_0}{\partial x} - \theta_x, \frac{\partial w_0}{\partial y} - \theta_y\right]^T \end{aligned} \tag{15}$$

are the generalized strain vectors due to membrane, bending and transverse shear deformation effects, respectively, and

$$\mathbf{S} = \begin{bmatrix} \mathbf{I}_3 & -z\mathbf{I}_3 & \mathbf{0}_{3\times2} \\ \mathbf{0}_{2\times3} & \mathbf{0}_{2\times3} & \mathbf{I}_2 \end{bmatrix} \tag{16}$$

is the generalized strain $\hat{\varepsilon}$ to the actual strain ε transformation matrix.

Now, let us consider a composite laminated plate formed by a stacking of n_l orthotropic layers with orthotropic axes 1, 2, 3 and isotropy in the 1 axis (i.e. in the plane 23). The 1 axis defines the direction of the longitudinal fibres which are embedded in a matrix of polymeric or metallic material. The relationships between the in-plane stresses $\sigma_p = [\sigma_x, \sigma_y, \tau_{xy}]^T$ and the transverse shear stresses $\sigma_s = [\tau_{xz}, \tau_{yz}]^T$ with their conjugate strains for each layer k can be written as

$$\sigma = \begin{pmatrix} \sigma_p \\ \sigma_s \end{pmatrix} = \begin{bmatrix} \mathbf{D}_p & \mathbf{0} \\ \mathbf{0} & \mathbf{D}_s \end{bmatrix} \begin{pmatrix} \varepsilon_p \\ \varepsilon_s \end{pmatrix} = \mathbf{D}\varepsilon \tag{17}$$

The constitutive matrices $\mathbf{D}_p$ and $\mathbf{D}_s$ are symmetrical and their terms are a function of independent material parameters and the angle β_k, and they can be obtained through

$$\mathbf{D}_p = \mathbf{T}_1^T \mathbf{D}_1 \mathbf{T}_1, \quad \mathbf{D}_s = \mathbf{T}_2^T \mathbf{D}_2 \mathbf{T}_2 \tag{18}$$

with $\mathbf{T}_1$ and $\mathbf{T}_2$ are coordinate transformation matrix from material principal coordinate system to global system, and $\mathbf{D}_1$ and $\mathbf{D}_2$ are in-plane constitutive matrix and transverse shear constitutive matrix in material principal coordinate system.

Now we are ready to establish the stress-strain relation between laminate stress and strain by integrating through the thickness of the laminate of the stress, we have

$$\hat{\sigma} = \hat{\mathbf{D}}\hat{\varepsilon} \tag{19}$$

with

$$\hat{\sigma} = \begin{pmatrix} \hat{\sigma}_m \\ \hat{\sigma}_b \\ \hat{\sigma}_s \end{pmatrix}, \quad \hat{\mathbf{D}} = \begin{bmatrix} \hat{\mathbf{D}}_m & \hat{\mathbf{D}}_{mb} & \mathbf{0}_{3\times 2} \\ \hat{\mathbf{D}}_{mb} & \hat{\mathbf{D}}_b & \mathbf{0}_{3\times 2} \\ \mathbf{0}_2 & \mathbf{0}_2 & \hat{\mathbf{D}}_s \end{bmatrix}$$

and

$$\hat{\sigma}_m = \int_{-t/2}^{t/2} \sigma_p dt \quad \hat{\sigma}_b = -\int_{-t/2}^{t/2} z\sigma_p dt \quad \hat{\sigma}_s = \int_{-t/2}^{t/2} \sigma_s dt$$

where $-t/2$ and $t/2$ are the z-coordinates of the lamina's upper and lower surfaces, respectively.

For a laminate with n_l orthotropic layers and homogeneous material within each layer we can write

$$\hat{\mathbf{D}}_m = \sum_{k=1}^{n_l} t_k \mathbf{D}_{p_k} \quad \hat{\mathbf{D}}_{mb} = \sum_{k=1}^{n_l} t_k \bar{z}_k \mathbf{D}_{p_k}$$
$$\hat{\mathbf{D}}_b = \sum_{k=1}^{n_l} \frac{1}{3}\left[z_{k+1}^3 - z_k^3\right] \mathbf{D}_{p_k} \tag{20}$$

where $t_k = z_{k+1} - z_k$, $\bar{z}_k = \frac{1}{2}(z_{k+1} + z_k)$ and $\mathbf{D}_{p_k}$ is the in-plane constitutive matrix for the kth layer.

The principle of virtual work (PVW) is written in terms of the generalized strains, the resultant stresses and the external distributed load $\mathbf{t}$ as

$$\int_A \delta\hat{\varepsilon}^T \hat{\sigma} dA = \int_A \delta\mathbf{u}^T \mathbf{t} dA \tag{21}$$

where A is the mid-plane surface of the plate, $\delta\mathbf{u} = [\delta u_0, \delta v_0, \delta w_0, \delta\theta_x, \delta\theta_y]^T$ and $\mathbf{t} = [f_x, f_y, f_z, m_x, m_y]^T$.

Considering the uncertainties in material properties, $\mathbf{b}$, constitutive matrix $\hat{\mathbf{D}}$ and the structural response $\mathbf{u}$ are stochastic function of $\mathbf{b}$. Using Taylor series expansion based perturbation approach to approximate the stochastic terms $\hat{\mathbf{D}}$, $\mathbf{u}$ and $\hat{\varepsilon}$, and retaining the second-order accuracy, then the zeroth-, first- and second-order equations of Eq.(21) can be written as follows (Kleiber and Hien, 1992):

The zeroth order

$$\int_A \delta\hat{\varepsilon}^T \hat{\mathbf{D}}\left(\bar{\mathbf{b}}\right) \hat{\varepsilon}\left(\bar{\mathbf{b}}\right) dA = \int_A \delta\mathbf{u}^T \mathbf{t}\left(\bar{\mathbf{b}}\right) dA \tag{22}$$

The first order

$$\sum_{i=1}^{n} \left\{ \int_A \delta\hat{\varepsilon}^T \hat{\mathbf{D}}\left(\bar{\mathbf{b}}\right) \left[D_{b_i} \hat{\varepsilon}\left(\bar{\mathbf{b}}\right)\right] dA - \int_A \delta\mathbf{u}^T \left[D_{b_i} \mathbf{t}\left(\bar{\mathbf{b}}\right)\right] dA + \int_A \delta\hat{\varepsilon}^T \left[D_{b_i} \hat{\mathbf{D}}\left(\bar{\mathbf{b}}\right)\right] \hat{\varepsilon}\left(\bar{\mathbf{b}}\right) dA \right\} \delta b_i = 0 \tag{23}$$

The second order

$$\sum_{i=1}^{n}\sum_{j=1}^{n} \left\{ \int_A \delta\hat{\varepsilon}^T \hat{\mathbf{D}}\left(\bar{\mathbf{b}}\right) \left[H_{b_i b_j} \hat{\varepsilon}\left(\bar{\mathbf{b}}\right)\right] dA - \int_A \delta\hat{\varepsilon}^T \left[H_{b_i b_j} \hat{\mathbf{D}}\left(\bar{\mathbf{b}}\right)\right] \hat{\varepsilon}\left(\bar{\mathbf{b}}\right) dA - 2\int_A \delta\hat{\varepsilon}^T \left[D_{b_i} \hat{\mathbf{D}}\left(\bar{\mathbf{b}}\right)\right] \left[D_{b_j} \hat{\varepsilon}\left(\bar{\mathbf{b}}\right)\right] dA - \int_A \delta\mathbf{u}^T \left[H_{b_i b_j} \mathbf{t}\left(\bar{\mathbf{b}}\right)\right] dA \right\} \delta b_i \delta b_j = 0 \tag{24}$$

3. FINITE ELEMENT IMPLEMENTATION

3.1. Finite element approximation of $\bar{\mathbb{C}}$

Using standard notations as follows,

$$\tilde{\mathbf{u}}_\mu = \mathbf{N}\tilde{\mathbf{a}}_\mu, \quad \nabla^s\tilde{\mathbf{u}}_\mu = \mathbf{B}\tilde{\mathbf{a}}_\mu, \quad \eta = \mathbf{N}\delta\mathbf{a}, \quad \nabla^s\eta = \mathbf{B}\delta\mathbf{a} \quad \text{and} \quad \varepsilon = \mathbf{B}\mathbf{a}^*,$$

where $\mathbf{N}$ denotes shape function, $\mathbf{B}$ is the strain-displacement matrix, $\tilde{\mathbf{a}}_\mu$ is nodal displacement fluctuation vector, $\delta\mathbf{a}$ is virtual nodal displacement fluctuation vector, $\mathbf{a}^*$ denotes the given nodal displacement vector. The finite element approximation to the zeroth-, first- and second-order variational principles in Eqs.(9-11), respectively are obtained as:

The zeroth-order

$$\left\{\mathbf{K}\tilde{\mathbf{a}}_\mu + \mathbf{K}\mathbf{a}^*\right\}\cdot\delta\mathbf{a} = \mathbf{0} \tag{25}$$

The first-order

$$\left\{\sum_{p=1}^{n}\left\{\mathbf{K}\left[D_{b_p}\tilde{\mathbf{a}}_\mu\right] + \left[D_{b_p}\mathbf{K}\right]\tilde{\mathbf{a}}_\mu + \left[D_{b_p}\mathbf{K}^{,p}\right]\mathbf{a}^*\right\}\delta b_p\right\}\cdot\delta\mathbf{a} = \mathbf{0} \tag{26}$$

The second-order

$$\left\{\sum_{p=1}^{n}\sum_{q=1}^{n}\left\{\mathbf{K}\left[H_{b_pb_q}\tilde{\mathbf{a}}_\mu\right] + \left[H_{b_pb_q}\mathbf{K}\right]\tilde{\mathbf{a}}_\mu + 2\left[D_{b_p}\mathbf{K}\right]\left[D_{b_p}\tilde{\mathbf{a}}_\mu\right] + \left[H_{b_pb_q}\mathbf{K}\right]\mathbf{a}^*\right\}\delta b_p\delta b_q\right\}\cdot\delta\mathbf{a} = \mathbf{0} \tag{27}$$

with $\mathbf{K} = \int_{\Omega_\mu^s}\mathbf{B}^T\mathbb{C}_\mu\mathbf{B}dV$, $\left[D_{b_p}\mathbf{K}\right] = \int_{\Omega_\mu^s}\mathbf{B}^T\left[D_{b_p}\mathbb{C}_\mu\right]\mathbf{B}dV$, and $\left[H_{b_pb_q}\mathbf{K}\right] = \int_{\Omega_\mu^s}\mathbf{B}^T\left[H_{b_pb_q}\mathbb{C}_\mu\right]\mathbf{B}dV$ denoted as the stiffness matrix and its first- and second-order partial derivatives, respectively. The solutions for microstructure displacement fluctuation field $\tilde{\mathbf{a}}_\mu$ and its derivatives $\left[D_{b_p}\tilde{\mathbf{a}}_\mu\right]$ and $\left[H_{b_pb_q}\tilde{\mathbf{a}}_\mu\right]$ can be found by introducing appropriate boundary conditions for the microstructure such as the three classic boundary conditions of linear displacement, periodic displacement and anti-periodic traction, and constant tractions. Details can be found in Zhou et al. (2014). With these at hand, the constitutive relation between the applied macrostrain $\bar{\varepsilon}$ and the homogenized macrostress $\bar{\sigma}$ can be calculated:

$$\bar{\mathbb{C}} = \frac{\bar{\sigma}}{\bar{\varepsilon}} \tag{28}$$

and similarly for its first- and second-order partial derivatives $\left[D_{b_i}\bar{\mathbb{C}}\right]$ and $\left[H_{b_ib_j}\bar{\mathbb{C}}\right]$, respectively.

3.2. Finite element formulation for laminated composite plates

Again, the finite element implementation to analyze the laminated composite plates can be obtained by introducing a conventional finite element discretization in Eqs.(22-24). Then their finite element approximations can be written as:

The zeroth order

$$\mathbf{K}\mathbf{u} = \mathbf{F} \tag{29}$$

The first order

$$\sum_{i=1}^{n}\left\{\mathbf{K}\left[D_{b_i}\mathbf{u}(\bar{\mathbf{b}})\right] + \left[D_{b_i}\mathbf{K}\right]\mathbf{u} - \left[D_{b_i}\mathbf{F}\left(\bar{\mathbf{b}}\right)\right]\right\}\delta b_i = 0 \tag{30}$$

The second order

$$\sum_{i=1}^{n}\sum_{j=1}^{n}\left\{\left[H_{b_ib_j}\mathbf{K}\left(\bar{\mathbf{b}}\right)\right] - \left[H_{b_ib_j}\mathbf{F}\left(\bar{\mathbf{b}}\right)\right] - 2\left[D_{b_i}\mathbf{K}\left(\bar{\mathbf{b}}\right)\right]\left[D_{b_j}\mathbf{u}\left(\bar{\mathbf{b}}\right)\right] - \left[H_{b_ib_j}\mathbf{K}\left(\bar{\mathbf{b}}\right)\right]\mathbf{u}\right\}\delta b_i\delta b_j = 0 \tag{31}$$

with $\mathbf{K} = \int_A\mathbf{B}^T\hat{\mathbf{D}}\mathbf{B}dA$, $\left[D_{b_i}\mathbf{K}\right] = \int_A\mathbf{B}^T\left[D_{b_i}\hat{\mathbf{D}}\right]\mathbf{B}dA$, and $\left[H_{b_ib_j}\mathbf{K}\right] = \int_A\mathbf{B}^T\left[H_{b_ib_j}\hat{\mathbf{D}}\right]\mathbf{B}dA$ denoted as the stiffness matrix of laminated plate elements and its first- and second-order partial derivatives, respectively. Solving the Eqs.(29-31) consecutively, the nodal displacements $\mathbf{u}$ and its first- and second-order partial derivatives, $\left[D_{b_i}\mathbf{u}\right]$ and $\left[H_{b_ib_j}\mathbf{u}\right]$ can be obtained, and other structural response terms can be calculated straightforwardly.

It should be noted that the stiffness matrix $\hat{\mathbf{D}}$ and its derivatives $\left[D_{b_i}\hat{\mathbf{D}}\right]$ and $\left[H_{b_ib_j}\hat{\mathbf{D}}\right]$ in the above Eqs.(29-31) are obtained by Eq.(28) through stochastic homogenization method. According to the first-order shear deformation theory, the through

thickness direction stress of the k-th ply σ_3 is assumed to be zero. A reduced stress-strain relation can be obtained from the stiffness matrix Eq.(28) as $\sigma = \mathbf{Q}\varepsilon$ with

$$Q_{ij} = \bar{\mathbb{C}}_{ij} - \frac{\bar{\mathbb{C}}_{i3}\bar{\mathbb{C}}_{j3}}{\bar{\mathbb{C}}_{33}}, \quad i,j = 1,2,6 \tag{32}$$

Hence, the in-plane and transverse shear stiffness matrix in Eq.(18) are

$$\mathbf{D}_1 = \begin{bmatrix} Q_{11} & Q_{12} & Q_{16} \\ Q_{21} & Q_{22} & Q_{26} \\ Q_{61} & Q_{62} & Q_{66} \end{bmatrix} \quad \mathbf{D}_2 = \begin{bmatrix} \bar{\mathbb{C}}_{44} & \bar{\mathbb{C}}_{45} \\ \bar{\mathbb{C}}_{54} & \bar{\mathbb{C}}_{55} \end{bmatrix}.$$

4. NUMERICAL EXAMPLE

For the demonstration of adequacy of the proposed approach, we analysed a square laminated composite plate. The dimension of the structure is given in Fig.1a. The plate is made of 4 graphite/epoxy unidirectional lamina with material properties listed in Table 1. The stacking sequence for respective lamina is $(30/-30)_4$ as an angle ply laminate, where the subscript 4 denotes the number of repetitions. The thickness of the lamina is assumed to be 5 mm. The structure is subject to a uniformly distributed load of $1000.0N/m^2$ or $1 \times 10^{-3}N/mm^2$, and the edges are simply supported.

Table 1: Statistical properties of random variables

Random variable	Symbol	Value
Fibre		
Axial modulus	E_z	233 GPa
Transverse modulus	E_p	23.1 GPa
Axial Poisson ratio	ν_z	0.2
Transverse Poisson ratio	ν_p	0.4
Axial shear modulus	G_z	8.96 Gpa
Matrix		
Young's modulus	E_m	4.62 GPa
Poisson ratio	ν_m	0.36 GPa

The response of the material at microscale level is analysed using representative volume element (RVE) with width l. In general, the width l is much smaller than the characteristic thickness of the laminae. The fibre-reinforced material is assumed to have periodic arrangement of finescale fibres embedded in a polymer matrix as shown in Fig.1b. A cubic RVE sample is shown in Fig.1c for a composite with hexagonal arrangements of unidirectional fibres. A local Cartesian coordinate system (1-2-3) is introduced at the microscale and oriented such 1-axis is aligned parallel to the axis of the fibres.

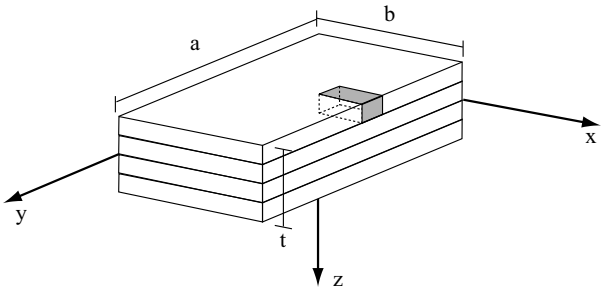

(a) Plate

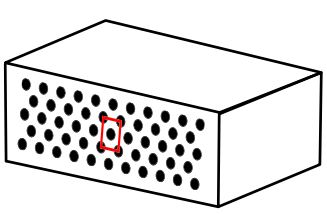

(b) Detail of fibres arrangement

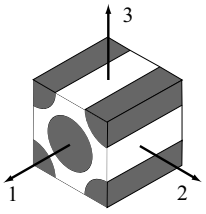

(c) RVE

Figure 1: Example of laminated fibre-reinforced composite plate

To calculate the effective stiffness matrix of the represented fibre-reinforced composite, the RVE has been meshed into 6263 four-node tetrahedral elements consisting of 4206 elements for fibres and 2057 elements for matrix, with a total of 1441 nodes. Implementing Eqs.(25-27) on the MoFEM (mesh-oriented finite element method) program (Kaczmarczyk et. al., 2014), the effective elastic tensor and its first- and second-order derivatives can be obtained through Eq.(28) for specified boundary condition. Here the effective constitutive model obtained under periodic displacement and anti-periodic traction boundary condition case are presented.

With the obtained effective stiffness matrix of each lamina, the reduced stiffness matrix and its first- and second-order partial derivatives can be obtained through Eq.(32). Introducing a certain type of element, the stochastic finite element analysis for the laminated plate can be conducted based on Eqs.(30-31). In the present study, the plate is

discretized into 12×12 four-node rectangular elements.

To demonstrate the accuracy of the present dual SFEM method, a comparison between the present approach and Monte Carlo simulation method (MCS) with 5000 samples has been performed. Uncertainty in the axial modulus of fibre, E_z were considered and various coefficients of variation ranged from 0.025 to 0.15 were examined. Results are shown in Fig 2 for the effective elastic properties with CoV of 0.15 for E_z, and Fig.3 for the deflection at the centre of the plate.

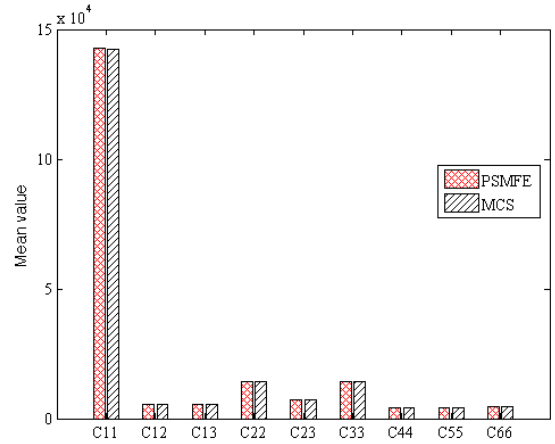

(a) Mean value

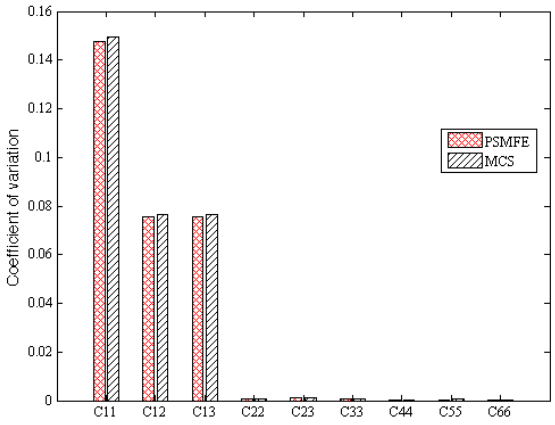

(b) Coefficient of variation

Figure 2: Statistics of the components of the effective elastic property due to variation in axial modulus of fibre, E_z, with CoV of 0.15

In general, Fig 2 and Fig.3 show good agreement between the present approach and MCS on the results of mean value and coefficient of variation with respect to various CoVs of E_z. This indicates that the numerical accuracy of the present dual SFEM is sufficient.

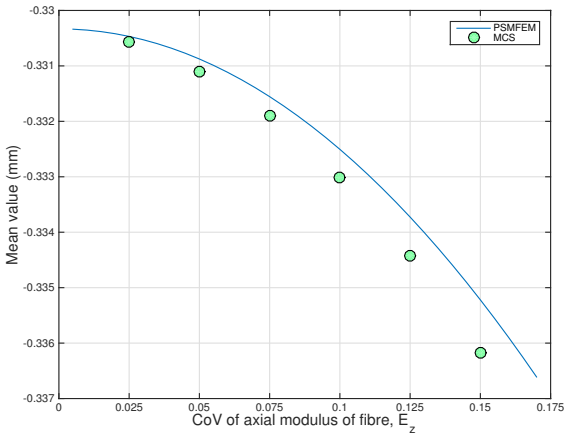

(a) Mean value

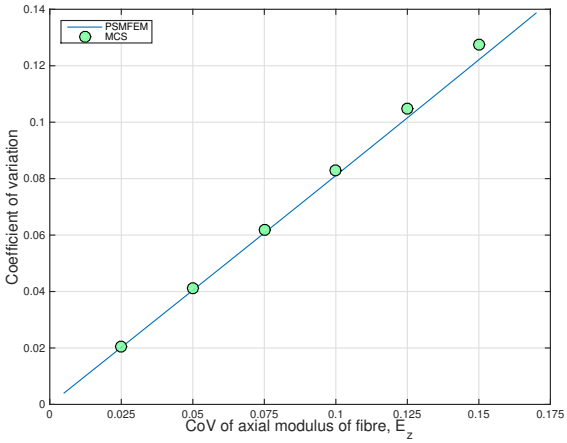

(b) Coefficient of variation

Figure 3: Statistics of the deflection at the centre of the plate w.r.t. various coefficients of variation in axial modulus of fibre, E_z

5. CONCLUSIONS

A dual stochastic finite element formulation taking into account the multi-layer effect and the microscopic variability of material properties in each lamina was developed for stochastic analysis of laminated composite plates. Stochastic homogenization method was used to propagate microscopic uncertainties. A comparison with Monte-Carlo simulation on the numerical accuracy shows that the proposed approach could provide reasonable probabilistic prediction.

ACKNOWLEGEMENT

The authors gratefully acknowledge the financial support provided for this study by the UK Engineering and Physical Sciences Research Council (EPSRC) under grant reference EP/K026925/1.

REFERENCES

Chamis, C. C. (2004). "Probabilistic simulation of multi-scale composite behavior." *Theoretical and Applied Fracture Mechanics*, 41(1–3), 51–61.

Charmpis, D. C., Schuëller, G. I., and Pellissetti, M. F. (2007). "The need for linking micromechanics of materials with stochastic finite elements: A challenge for materials science." *Computational Materials Science*, 41(1), 27–37.

Chen, N.-Z. and Guedes Soares, C. (2008). "Spectral stochastic finite element analysis for laminated composite plates." *Computer Methods in Applied Mechanics and Engineering*, 197(51–52), 4830–4839.

Chuang, S.-N. (2006). "Probabilistic analysis for the mechanical properties of cross-ply fiber-reinforced composite laminate." *ASME 2006 International Mechanical Engineering Congress and Exposition*, 171–183.

Frangopol, D. M. and Recek, S. (2003). "Reliability of fiber-reinforced composite laminate plates." *Probabilistic Engineering Mechanics*, 18(2), 119–137.

Jeong, H. K. and Shenoi, R. A. (2000). "Probabilistic strength analysis of rectangular frp plates using monte carlo simulation." *Computers & Structures*, 76(1–3), 219–235.

Kaczmarczyk et. al. (2014). *Mesh Oriented Finite Element Method (MoFEM), Version 0.1.4*. University of Glasgow, Glasgow, UK, <https://bitbucket.org/likask/mofem-joseph/wiki/Home/>.

Kleiber, M. and Hien, T. D. (1992). *The stochastic finite element method - Basic perturbation technique and computer implementation*. John Wiley & Sons.

Matthies, H. G. (2007). *Uncertainty Quantification with Stochastic Finite Elements*. John Wiley & Sons, Ltd, book section 27, 1–36.

Motley, M. R. and Young, Y. L. (2011). "Influence of uncertainties on the response and reliability of self-adaptive composite rotors." *Composite Structures*, 94(1), 114–120.

Murotsu, Y., Miki, M., and Shao, S. (1994). "Reliability design of fiber reinforced composites." *Structural Safety*, 15(1–2), 35–49.

Ngah, M. F. and Young, A. (2007). "Application of the spectral stochastic finite element method for performance prediction of composite structures." *Composite Structures*, 78(3), 447–456.

Oñate, E. (2013). *Structural analysis with the finite element method linear statics: volume 2. beams, plates and shells*. Springer Netherlands.

Potter, K., Khan, B., Wisnom, M., Bell, T., and Stevens, J. (2008). "Variability, fibre waviness and misalignment in the determination of the properties of composite materials and structures." *Composites Part A: Applied Science and Manufacturing*, 39(9), 1343–1354.

Sasikumar, P., Suresh, R., and Gupta, S. (2014). "Analysis of cfrp laminated plates with spatially varying non-gaussian inhomogeneities using sfem." *Composite Structures*, 112(0), 308–326.

Schuëller, G. I. and Pradlwarter, H. J. (2009). "Uncertainty analysis of complex structural systems." *International Journal for Numerical Methods in Engineering*, 80(6-7), 881–913.

Soares, C. G. (1997). "Reliability of components in composite materials." *Reliability Engineering & System Safety*, 55(2), 171–177.

Sriramula, S. and Chryssanthopoulos, M. K. (2009). "Quantification of uncertainty modelling in stochastic analysis of frp composites." *Composites Part A: Applied Science and Manufacturing*, 40(11), 1673–1684.

Stefanou, G. (2009). "The stochastic finite element method: Past, present and future." *Computer Methods in Applied Mechanics and Engineering*, 198(9–12), 1031–1051.

Talha, M. and Singh, B. N. (2014). "Stochastic perturbation-based finite element for buckling statistics of fgm plates with uncertain material properties in thermal environments." *Composite Structures*, 108(0), 823–833.

Welemane, H. and Dehmous, H. (2011). "Reliability analysis and micromechanics: A coupled approach for composite failure prediction." *International Journal of Mechanical Sciences*, 53(11), 935–945.

Zhou, X.-Y., Gosling, P. D., Pearce, C. J., Kaczmarczyk, L., and Ullah, Z. (2014). "Perturbation-based stochastic multi-scale computational homogenization method for the determination of the effective properties of composite materials with random poperties." *Computer Methods in Applied Mechanics and Engineering*, under review.